

A Soluble Free-Fermion Model in d Dimensions

F. Y. Wu and H. Y. Huang

Department of Physics, Northeastern University, Boston, Massachusetts 02115

(October 17, 2018)

Abstract

We consider a vertex model in d dimensions characterized by lines which run in a preferred direction. We show that this vertex model is soluble if the weights of vertices with intersecting lines are given by a free-fermion condition, and that a fugacity -1 is associated to each loop of lines. The solution is obtained by mapping the model into a dimer problem and by evaluating a Pfaffian. We also determine the critical point and the singular behavior of the free energy.

PACS number: 05.50.+q

arXiv:cond-mat/9412022v2 9 Dec 1994

Typeset using REVTeX

I. INTRODUCTION

An outstanding unsolved problem in statistical mechanics has been the exact solution of lattice models in three or higher dimensions. While a host of lattice models has been solved in two dimensions [1], very few exact results are known for three or higher dimensions. Some two decades ago Suzuki [2] solved a three-dimensional Ising model with pure 4-spin interactions, which turns out to be a two-dimensional model in disguise. Similarly, a three-dimensional 5-edge model solved by Orland [3] is equivalent to a two-dimensional dimer problem [4]. The first exact solution of a genuine three-dimensional model was that obtained by Baxter [5] for the Zamolodchikov model [6], a 2-state interaction-round-a-cube (IRC) model involving some negative Boltzmann weights. Since then Baxter and Bazhanov [7] have further extended the solution to the IRC model of N states for general N . Very recently, we have solved a vertex model in arbitrary dimensionality [8]. This is a vertex model described by lines which run in a preferred direction on the lattice and do not intersect. Like the three-dimensional IRC model of Refs. [5] and [6], this model also involves negative Boltzmann weights. While the nonintersecting feature makes it possible to use this model to describe flux lines in type II superconductors [9], the more general version of the model with vertices of intersecting lines remains unsolved.

Some twenty-five years ago one of us and Fan [10,11] introduced the term *free-fermion model* to lattice-statistical vertex models satisfying a certain free fermion condition. When this condition holds, the model can be regarded as one describing free fermions on a lattice [8] and becomes soluble. But soluble free-fermion models have been restricted mainly to two dimensions [12]. In this paper we extend the solution of [8] to a free fermion model which includes vertices of intersecting lines in any dimension. This yields a new class of soluble free fermion models in arbitrary dimensionality.

II. THE MODEL

In the vertex models considered in [8], vertex configurations are described by lines embedded on a lattice subject to:

- i) lines do not intersect,
- ii) lines are oriented in a preferred direction, and
- iii) each loop of line possesses a fugacity -1 .

Now we relax condition (i) by allowing lines to intersect. For definiteness we consider a Cartesian lattice \mathcal{L} in d dimensions. Place bonds along edges of \mathcal{L} with the restriction that the number of bonds incident at each vertex is zero or even, with half of the bonds incident in the positive and the other half in the negative axes directions. The bonds then form lines which run along the main diagonal of \mathcal{L} . Thus, we have a D -vertex model with D different vertex configurations, where

$$D = \sum_{r=0}^d \binom{d}{r}^2 = \binom{2d}{d}, \quad (1)$$

where r is the number of lines intersecting at the vertex. This leads to $D = 6, 20, \dots$ for $d = 2, 3, \dots$, respectively.

Number the negative axes incident at a vertex $\{n\} = \{1, 2, \dots, d\}$ and the positive incident axes $\{p\} = \{d+1, d+2, \dots, 2d\}$, such that $\{i, d+i\}$ refer to the axis in the i th direction. Denote by $\omega_{\{n'\}\{p'\}}$ the weight of a vertex with bonds (lines) incident at $\{n'\} \in \{n\}$ and $\{p'\} \in \{p\}$. For vertices with no incident bonds we take the weight $\omega_0 = 1$, and for vertices with two incident bonds, one in the negative direction i and one in the positive direction j , we take the weight to be ω_{ij} . For vertices with four or more bonds the weights are given by the free-fermion condition

$$\begin{aligned} \omega_{\{n'\}\{p'\}} &= \sum_P (-1)^{\delta_P} \prod_{i \in \{n'\}, j \in \{p'\}} \omega_{ij} \\ &= \det|\omega_{ij}|, \end{aligned} \quad (2)$$

where the summation is taken over all pairings P of axes into pairs $\{ij\}$, $i \in \{n'\}$ and

$j \in \{p'\}$, and δ_P is the signature of P , the number of transposition needed to bring the indices of the pairing to the *canonical ordering*

$$\{1, d+1\}\{2, d+2\} \cdots \{d, 2d\}. \quad (3)$$

Here, it is understood that indices not contained in $\{n'\}$ and $\{p'\}$ are deleted in (3) in determining the canonical ordering. For $d = 3$, for example, (2) gives

$$\begin{aligned} \omega_{1245} &= \omega_{14}\omega_{25} - \omega_{15}\omega_{24} \\ \omega_{1256} &= \omega_{16}\omega_{25} - \omega_{15}\omega_{26} \\ \omega_{1246} &= \omega_{14}\omega_{26} - \omega_{16}\omega_{24}, \end{aligned} \quad (4a)$$

for $\{n'\} = \{12\}$, and other similar relations for $\{n'\} = \{13\}, \{23\}$, and

$$\begin{aligned} \omega_{123456} &= \omega_{14}\omega_{25}\omega_{36} + \omega_{15}\omega_{26}\omega_{34} + \omega_{16}\omega_{24}\omega_{35} \\ &\quad - \omega_{14}\omega_{26}\omega_{35} - \omega_{15}\omega_{24}\omega_{36} - \omega_{16}\omega_{25}\omega_{34}, \end{aligned} \quad (4b)$$

for $\{n'\} = \{n\} = \{123\}$. Note that the expression (2) can be written as a determinant as indicated. The model considered in [8] corresponds to taking $\omega_{ij} = \sqrt{z_i z_j}$, $z_i = z_{i+d}$ so that the weights (4a) and (4b) vanish identically, indicating that vertices with 4 or more bonds are forbidden.

The vertex weight (2) can be represented graphically by decomposing the vertex configuration into continuous lines indicated by the pairings. That is, for each ω_{ij} one connects the negative axis i to the positive axis j . For the vertex weight (4b), for example, this leads to the graphs shown in Fig. 1. In this picture and assuming periodic boundary conditions, lines form loops wound around the lattice. Let ℓ be the overall number of loops when each vertex configuration is decomposed into its canonical ordering. This permits us to define a partition function

$$Z = \sum_{\text{vertex config.}} (-1)^\ell \prod_{\text{vertex}} \omega_{\{n'\}\{p'\}}. \quad (5)$$

Now, substitute (2) into (5) and observe that when all pairings are in the order of the canonical form we have $\delta_P = 0$, and whenever the pairing of two lines interchanges at a

vertex, such as changing $\{14, 25\}$ to $\{15, 24\}$ in the first line of (4a), both ℓ and δ_P change by 1. It follows that we can rewrite the partition function (5) as

$$Z = \sum_{\text{loop config.}} (-1)^\ell \prod \omega_{ij}, \quad (6)$$

where the summation is taken over all possible loop configurations of ℓ loops, and the product is taken over all ω_{ij} factors only, which are present along the loops. In the next section we show that, in the form of (6), the partition function Z is precisely a dimer generating function.

III. A DIMER PROBLEM

Introduce a dimer lattice \mathcal{L}' by expanding every lattice point of \mathcal{L} into a “city”, which we choose to be the one consisting of $2d$ points located on the $2d$ incident axes $\{n\}$ and $\{p\}$. The situation of $d = 3$ is shown in Fig. 2. Let N and $2dN$ be the respect numbers of lattice points in \mathcal{L} and \mathcal{L}' . Connect as shown in Fig. 2 each point in $\{n\}$ to every point in $\{p\}$, and vice versa. There are now two kinds of edges in \mathcal{L}' : intercity edges connecting cities and intracity edges within a city. Starting from a given vertex configuration on \mathcal{L} , we cover each intercity edge on \mathcal{L}' by a dimer (resp. leave it empty) if the corresponding edge on \mathcal{L} is empty (resp. covered by a bond). The remaining uncovered points on \mathcal{L}' are then covered by dimers placed along intracity edges. This latter covering corresponds to the different pairings of the remaining points and is generally not unique. For example, the different coverings corresponding to ω_{1245} and ω_{123456} given by (4a) and (4b) together with the associated signs are shown in Fig. 3. In this way, we have mapped vertex configurations into dimer coverings.

We now establish that there is a one-one correspondence between dimer coverings of \mathcal{L}' and loop configurations in (6). Consider first dimer coverings on \mathcal{L}' . Superimpose any given dimer covering C_i with a standard one, C_0 , in which all intercity edges are covered by dimers. The superposition of two dimer coverings produces a graph of transition cycles, or polygons

[13]. In the present case, the transition cycles belong to one of two kinds: double dimers placed on intercity edges, and polygons wound around the lattice forming loops. Thus, each dimer covering is mapped into a loop configuration. Conversely, to each loop configuration in (6), there exists a unique dimer covering C_i which, when superimposed upon C_0 , produces the loop configuration in question. This completes the proof.

It is well-known that dimer coverings are generated by a Pfaffian, provided signs can be fixed correctly [13]. In the usual dimer problem all terms in the dimer generating function have the same sign, and for this reason the generating function can be written as a Pfaffian only for planar lattices. In the present case, however, the partition function (6) is precisely a Pfaffian as we now see.

Number the $2dN$ lattice points of \mathcal{L}' in the increasing order along the main diagonal of \mathcal{L} , and within a city in the order as shown in Fig. 2. Direct all intercity edges of \mathcal{L}' in the positive direction and all intracity edges of \mathcal{L}' as shown in Fig. 2. In this way all edges are directed in the positive directions. Further, the factor $\prod \omega_{ij}$ in (6) is generated by taking the dimer weight 1 for intercity edges and weights $\omega_{ij}, i < j$, for intracity edges. To fix the sign associated with this product, we consider a typical term in the Pfaffian corresponding to the dimer configuration C_i . The sign of this term relative to the term corresponding to C_0 is the product of the signs of the transition cycles produced by the superimposition of C_i and C_0 [13]. The rule is that each transition cycle carries a sign $(-1)^{n+1}$, where n is the number of arrows pointing in a given direction when the transition cycle is traversed. For transition cycles consisting of double dimers we have $n = 1$ so that the sign is always positive. For transition cycles consisting of loops around the lattice we have, since all edges are directed in the same direction, $n = \text{even}$, so that the sign is always negative for each loop. Then the overall sign of C_i relative to C_0 is $(-1)^\ell$. This establishes that the partition function (6) is precisely a Pfaffian.

IV. EVALUATION OF THE PARTITION FUNCTION

We now evaluate the Pfaffian.

Let $N = N_1 \times N_2 \times \cdots \times N_d$, where N_i be the linear dimensions of \mathcal{L} . Then the Pfaffian is the square root of the determinant of a $2dN \times 2dN$ antisymmetric matrix \mathbf{A} in the form of a direct product of $2d \times 2d$ matrices indexed by

$$\begin{aligned}
 \mathbf{A}(n_1, \dots, n_d | n_1, \dots, n_d) &= \begin{pmatrix} \mathbf{0} & \mathbf{W} \\ -\mathbf{W} & \mathbf{0} \end{pmatrix} \\
 \mathbf{A}(n_1, \dots, n_i, \dots, n_d | n_1, \dots, n_i + 1, \dots, n_d) &= \begin{pmatrix} \mathbf{0} & \mathbf{U}_i \\ \mathbf{0} & \mathbf{0} \end{pmatrix} \\
 \mathbf{A}(n_1, \dots, n_i, \dots, n_d | n_1, \dots, n_i - 1, \dots, n_d) &= \begin{pmatrix} \mathbf{0} & \mathbf{0} \\ -\mathbf{U}_i & \mathbf{0} \end{pmatrix} \\
 \mathbf{A}(m_1, \dots, m_d | n_1, \dots, n_d) &= \begin{pmatrix} \mathbf{0} & \mathbf{0} \\ \mathbf{0} & \mathbf{0} \end{pmatrix}, \quad \text{otherwise}
 \end{aligned} \tag{7}$$

where $\mathbf{0}$ is the d -dimensional zero matrix, \mathbf{W} a $d \times d$ matrix with elements $W_{ij} = \omega_{i,j+d}$, and \mathbf{U}_i a $d \times d$ matrix whose only nonzero element is $\{U_i\}_{ii} = 1$.

With periodic boundary conditions, matrices in (7) are invariant when indices m_i, n_i are changed by N_i . Then the matrix is block-diagonal in the Fourier space. This leads to the following expression for the partition function

$$\begin{aligned}
 Z &= \sqrt{\det \mathbf{A}} \\
 &= \prod_{n_1=1}^{N_1} \cdots \prod_{n_d=1}^{N_d} \left[\det \begin{pmatrix} \mathbf{0} & \mathbf{B} \\ -\mathbf{B}^* & \mathbf{0} \end{pmatrix} \right]^{1/2} \\
 &= \prod_{n_1=1}^{N_1} \cdots \prod_{n_d=1}^{N_d} \det |\mathbf{B}|,
 \end{aligned} \tag{8}$$

where $\mathbf{B} \equiv \mathbf{B}(2\pi n_1/N_1, \dots, 2\pi n_d/N_d)$ is a $d \times d$ matrix with elements

$$\begin{aligned}
 B_{ij} &= \omega_{i,j+d}, & i \neq j \\
 &= \omega_{i,i+d} + e^{2\pi i n_i/N_i}, & i = j, \quad i, j = 1, \dots, d,
 \end{aligned} \tag{9}$$

and \mathbf{B}^* is the complex conjugate of \mathbf{B} . In this way, we obtain the per-site free energy

$$\begin{aligned} f_d &= \lim_{N_i \rightarrow \infty} N^{-1} \ln Z \\ &= \frac{1}{(2\pi)^d} \int_0^{2\pi} d\theta_1 \cdots \int_0^{2\pi} d\theta_d \ln |D_d(\theta_1, \dots, \theta_d)|, \end{aligned} \quad (10)$$

where

$$D_d(\theta_1, \dots, \theta_d) = \det\{\mathbf{B}(\theta_1, \dots, \theta_d)\}, \quad (11)$$

Particularly, for $d = 2$ and 3 , we have

$$\begin{aligned} D_2(\theta_1, \theta_2) &= \omega_{1234} + \omega_{24}e^{i\theta_1} + \omega_{13}e^{i\theta_2} + e^{i(\theta_1+\theta_2)}, \\ D_3(\theta_1, \theta_2, \theta_3) &= \omega_{123456} + \omega_{2356}e^{i\theta_1} + \omega_{1346}e^{i\theta_2} + \omega_{1245}e^{i\theta_3} \\ &\quad + \omega_{14}e^{i(\theta_2+\theta_3)} + \omega_{25}e^{i(\theta_1+\theta_3)} + \omega_{36}e^{i(\theta_1+\theta_2)} + e^{i(\theta_1+\theta_2+\theta_3)}. \end{aligned} \quad (12)$$

Here, the ω 's with 4 or more indices are those defined by (2) - (4b). Particularly, we have, in addition to those given in (4a) and (4b), $\omega_{2356} = \omega_{25}\omega_{36} - \omega_{26}\omega_{35}$, $\omega_{1346} = \omega_{14}\omega_{36} - \omega_{16}\omega_{34}$. Explicitly, $D_d(\theta_1, \dots, \theta_d)$ is a linear combination of terms in the form of $c_{ij\dots k}e^{i(\theta_i+\theta_j+\dots+\theta_k)}$, where the coefficient $c_{ij\dots k}$ is the determinant of the matrix \mathbf{W} with the i, j, \dots, k th rows and columns deleted. By taking $\omega_{ij} = \sqrt{z_i z_j}$, $z_i = z_{i+d}$ for which the free-fermion weights with 4 or more indices vanish identically, these results reduce to those of [8].

V. THE CRITICAL BEHAVIOR

For $d = 2$ the vertices are those of a six-vertex model shown in Fig. 4 with the weights

$$\begin{aligned} \Omega_1 &= 1, & \Omega_2 &= \omega_{1234} = \Omega_3\Omega_4 - \Omega_5\Omega_6 \\ \Omega_3 &= \omega_{13}, & \Omega_4 &= \omega_{24} \\ \Omega_5 &= \omega_{14}, & \Omega_6 &= \omega_{23}. \end{aligned} \quad (13)$$

Note that the free-fermion condition is now $\Omega_1\Omega_2 = \Omega_3\Omega_4 - \Omega_5\Omega_6$ and differs slightly (corresponding to the negation of Ω_2) from the usual form [9] $\Omega_1\Omega_2 = -\Omega_3\Omega_4 + \Omega_5\Omega_6$ for which

the partition function is defined by (5) without the loop factor $(-1)^\ell$. Rewriting (12) and carrying out one integration, say, over θ_2 , we have

$$\begin{aligned} f_2 &= \frac{1}{(2\pi)^2} \int_0^{2\pi} d\theta_1 \int_0^{2\pi} d\theta_2 \ln |\Omega_2 + \Omega_3 e^{i\theta_1} + \Omega_4 e^{i\theta_2} + \Omega_1 e^{i(\theta_1+\theta_2)}| \\ &= \frac{1}{2\pi} \int_0^{2\pi} d\theta_1 \ln \max \left\{ |\Omega_2 + \Omega_3 e^{i\theta_1}|, |\Omega_4 + \Omega_1 e^{i\theta_1}| \right\}. \end{aligned} \quad (14)$$

This free energy reduces to that of usual free-fermion 6-vertex model after negating Ω_2 [8]. The equivalence of the two free energies (with and without the loop factor) is a property unique to two dimensions.

When one of the two absolute values in (14) is larger than the other for all θ_1 , then one can carry out the remaining integration and obtains

$$f_2 = \max \{ |\Omega_1|, |\Omega_2|, |\Omega_3|, |\Omega_4| \}, \quad (15)$$

so that the system is in a "frozen" state. Now the two absolute values in (14) are linear in $\cos \theta_1$. As a consequence, when perturbed from the frozen states (15), the two absolute values will cross only at $\theta_1 = 0$ or π , near which one of the two absolute values is always larger. This leads to the two critical conditions

$$|\Omega_2 \pm \Omega_3| = |\Omega_4 \pm \Omega_1|, \quad (16)$$

at which f_2 becomes singular. Near the critical point say, $\Omega_2 + \Omega_3 = \Omega_4 + \Omega_1$ for all $\Omega_i > 0$, for instance, let

$$t = \Omega_2 + \Omega_3 - \Omega_4 - \Omega_1 \sim \text{small positive}. \quad (17)$$

Then, the singular part of f_2 is given by

$$\{f_2\}_{\text{sing}} = \frac{1}{2\pi} \int_{-\alpha(t)}^{\alpha(t)} d\theta_1 \ln \left| \frac{\Omega_2 + \Omega_3 e^{i\theta_1}}{\Omega_4 + \Omega_1 e^{i\theta_1}} \right|, \quad (18)$$

where $\alpha(t) > 0$ is determined from

$$|\Omega_2 + \Omega_3 e^{i\alpha}| = |\Omega_4 + \Omega_1 e^{i\alpha}|. \quad (19)$$

It is easy to verify that $\alpha \sim \sqrt{t}$, and for small t the integrand in (18) is of the order of $t + \theta_1^2$.

It follows that

$$\{f_2\}_{\text{sing}} \sim t^{3/2}. \quad (20)$$

The same critical behavior is deduced if any of the weights, say, Ω_2 , is negative.

The example of $d = 2$ serves to illustrate the origin of the critical behavior and the critical point. After carrying out one-fold integration, f_2 is given in the form of an integration of a competition of the logarithms of two absolute values as in the second line of (14). Then, the critical point is the point at which the two absolute values are equal and the integrand in (14) switches from one absolute value to the other for small deviations from the critical point. This creates a singularity in the free energy. We shall call this the switching property of the integrand. A prerequisite for switching to occur is that the ratio of the two absolute values is an extremum in θ_1 at the critical point. For $d = 2$ this can occur only at $\theta_1 = 0$ or π . This leads to a singular part of the free energy in the form of (18), where the integration is taken over a region \mathcal{R} whose boundary is determined by setting the two absolute values equal at fixed small deviation t from criticality. It follows that the singular behavior is that of this integral, namely, $tV(t)$, where $V(t) \sim \sqrt{t}$ (for $d = 2$) is the volume of \mathcal{R} .

Applying the same argument to $d \geq 3$, one first carries out one-fold integration over, say, θ_j , yielding f_d in the form of an integration of a competition of the logarithms of the absolute values of $A_j(\theta_\alpha)$, $\alpha \neq j$, the collection of terms in D_d linear in $e^{i\theta_j}$, and $B_j(\theta_\alpha)$, the collection of terms in D_d independent of $e^{i\theta_j}$. Then f_d can be singular at points in the parameter space at which the two absolute values become equal and possess the aforementioned switching and extremum property. Namely, there exist angles $\theta_{\alpha 0}$, $\alpha \neq j$, such that

$$|A_j(\theta_{\alpha 0})| = |B_j(\theta_{\alpha 0})|, \quad t = 0 \quad (21)$$

and

$$\begin{aligned} |A_j(\theta_\alpha)| &> |B_j(\theta_\alpha)|, & t < 0 \\ |A_j(\theta_\alpha)| &\leq |B_j(\theta_\alpha)|, & t = 0+ \end{aligned} \quad (22)$$

for θ_α in a neighborhood of $\theta_{\alpha 0}$, where t is the deviation from the critical point. (Here, the roles of A_j and B_j can be interchanged.) Since the integrand of the free energy switches from $|A_j|$ to $|B_j|$ for $t = 0+$, a singular part in the form of (18) appears in the free energy, which is the integration of $\ln |A_j/B_j|$ over a region \mathcal{R} bounded by

$$|A_j(\theta_\alpha)| = |B_j(\theta_\alpha)|, \quad t = \text{small fixed.} \quad (23)$$

The critical condition is now given by (21) and the critical behavior is $tV(t)$, where $V(t)$ is the volume of the $(d - 1)$ -dimensional region \mathcal{R} .

To determine $V(t)$, we expand $\ln |A_j/B_j|$ about $\theta_{\alpha 0}$ and $t = 0$, obtaining generally the leading behavior

$$ct + F(\Delta\theta_\alpha), \quad (24)$$

where c is a constant and $\Delta\theta_\alpha = \theta_\alpha - \theta_{\alpha 0}$. Here, due to the extremum property, F is a quadratic form in variables $\Delta\theta_\alpha$, which is either positive or negative definite. This implies that the region \mathcal{R} has linear dimensions $\Delta\theta_\alpha \sim t^{1/2}$, and hence $V(t) \sim t^{(d-1)/2}$. The singular part of the free energy behaves as

$$\{f_d\}_{\text{sing}} \sim t^{(d+1)/2}. \quad (25)$$

This is the critical behavior found in the model $\Omega_2 = 0$ [8]. The meaning of the singular behavior (25) for $d = \text{odd}$ is that the $[(d + 1)/2]$ -th derivative of f_d is discontinuous.

However, the singular behavior (25) may not be the dominate one. If the $(d - 1)$ -dimensional integral $\int \ln |A_j|$ dominant in (21) - (23) is also singular at $t = 0$, then the critical behavior of the free energy at $t = 0$ is that of a $(d - 1)$ -dimensional model. By the same token, the critical behavior can be reduced further to that of lower dimensions. Examples are given in the next section.

VI. EXAMPLES

A. Example 1

If lines in the vertex model are nonintersecting, then we have the model considered in [8] with

$$D_d(\theta_1, \dots, \theta_d) = 1 + \sum_{i=1}^d z_i e^{i\theta_i}. \quad (26)$$

There is no loss of generality in supposing $|z_i| \leq 1$. Carry out the integration in (10) over θ_1 , say, after rewriting D_d as $e^{-i\theta_1} + z_1 + z_2 e^{i\theta_2} + \dots + z_d e^{i\theta_d}$, where we have renamed $\theta_\alpha - \theta_1$ as θ_α . If any of the z_α is negative, one replaces θ_α by $\pi + \theta_\alpha$ and obtains $A_1 = 1$ and $B_1 = |z_1| + |z_2| e^{i\theta_2} + \dots + |z_d| e^{i\theta_d}$. It is then straightforward to verify that the extremum property occurs only at $\theta_{\alpha 0} = 0$, $\alpha = 2, \dots, d$. The critical point occurs at

$$|z_1| + |z_2| + \dots + |z_d| = 1, \quad (27)$$

and the critical behavior of the free energy is $t^{(d+1)/2}$.

B. Example 2

. Consider the 3-dimensional model with weights

$$\begin{aligned} \omega_{36} &= z, & \omega_{24} &= z_1/z \\ \omega_{16} &= \omega_{26} = z \\ \omega_{34} &= \omega_{35} = 1 \\ \omega_{14} &= \omega_{25} = \omega_{15} = 0 \end{aligned} \quad (28)$$

for z and z_1 real, implying, using (4a) and (4b),

$$\begin{aligned} \omega_{123456} &= z_1, & \omega_{1245} &= 0 \\ \omega_{1346} &= \omega_{2356} = -z. \end{aligned} \quad (29)$$

By appropriately changing integration variables, the per-site free energy (10) assumes the form

$$f_3 = \frac{1}{(2\pi)^3} \int_0^{2\pi} d\theta_1 \int_0^{2\pi} d\theta_2 \int_0^{2\pi} d\theta_3 \ln |z_1 + ze^{i\theta_1} + ze^{i\theta_2} + ze^{i(\theta_1+\theta_2)} + e^{i(\theta_1+\theta_2+\theta_3)}|. \quad (30)$$

After carrying out the integration over θ_3 , one obtains $A_3 = 1$, $B_3 = z_1 + ze^{i\theta_1} + ze^{i\theta_2} + ze^{i(\theta_1+\theta_2)}$ with

$$\begin{aligned} |B_3|^2 &= (z_1 + 3z)^2 + 2z(z + z_1)(\cos \theta_1 + \cos \theta_2 - 2) \\ &\quad + 2zz_1[\cos(\theta_1 + \theta_2) - 1] + 2z^2[\cos(\theta_1 - \theta_2) - 1]. \end{aligned} \quad (31)$$

It can be verified that $|B_3|$ possesses one extremum at $\theta_{10} = \theta_{20} = 0$ in the regimes $z_1/z > -1/3$ and $z_1/z < -3$, which, by setting the extremum equal to one, leads to the critical point

$$|z_1 + 3z| = 1. \quad (32)$$

Define $t = |z_1 + 3z| - 1$. Then one finds

$$\begin{aligned} f_3 &= 0, & t < 0 \\ \{f_3\}_{\text{sing}} &\sim t^2, & t = 0+ \end{aligned} \quad (33)$$

for $z_1/z > -1/3$, and

$$\begin{aligned} f_3 &= \ln |z_1|, & t > 0 \\ \{f_3\}_{\text{sing}} &\sim t^2, & t = 0-. \end{aligned} \quad (34)$$

for $z_1/z < -1/3$. In addition, another extremum occurs at $\cos \theta_{10} = \cos \theta_{20} = -(z_1 + z)/2z_1$ in the regime $|1 - 3z_1/z| > 2$, which leads to the critical point

$$(z_1 - z)^3 = z_1. \quad (35)$$

Define $t = |z_1 - z|^3 - |z_1|$. Then one finds the behavior (33) for $z_1/z < -1/3$ and (34) for $z_1/z > -1/3$. These results lead to the phase diagram shown in Fig. 5.

C. Example 3

Consider another 3-dimensional model with weights

$$\begin{aligned}
\omega_{15} &= z, & \omega_{36} &= -1 \\
\omega_{14} &= \omega_{25} = 0 \\
\omega_{24} &= \omega_{26} = \omega_{34} = \omega_{35} = \omega_{16} = 1
\end{aligned} \tag{36}$$

implying,

$$\begin{aligned}
\omega_{2356} &= \omega_{1346} = -1 \\
\omega_{1245} &= -z \\
\omega_{123456} &= 2z + 1.
\end{aligned} \tag{37}$$

The per-site free energy is

$$f_3 = \frac{1}{(2\pi)^3} \int_0^{2\pi} d\theta_1 \int_0^{2\pi} d\theta_2 \int_0^{2\pi} d\theta_3 \ln |2z + 1 - e^{i(\theta_1+\theta_2)} - e^{i\theta_1} - e^{i\theta_2} - ze^{i\theta_3} + e^{i(\theta_1+\theta_2+\theta_3)}| \tag{38}$$

After carrying out the integration over θ_3 , one obtains $A_3 = z - e^{i(\theta_1+\theta_2)}$, $B_3 = 2z + 1 - e^{i(\theta_1+\theta_2)} - e^{i\theta_1} - e^{i\theta_2}$, leading to the critical point

$$z = 1, \tag{39}$$

at $\theta_{10} = \theta_{20} = 0$. Define $t = z - 1$. It can be verify that $|A_3| \leq |B_3|$ for $t \geq 0$, and a switching from $|B_3|$ to $|A_3|$ occurs in a small regime in the neighborhood of $\theta_{10} = -\theta_{20}$, $t = 0-$. Hence the free energy contains a singular part of the order of $O(t^2)$ for $t = 0-$. However, it turns out that the dominate integral

$$f_3 \sim \frac{1}{(2\pi)^2} \int_0^{2\pi} d\theta_1 \int_0^{2\pi} d\theta_2 \ln |B_3(\theta_1, \theta_2)|, \tag{40}$$

is also singular at $t = 0$. As in (14), further integrations of (40) lead to the critical behavior

$$\begin{aligned}
f_3 &= \ln |2z + 1|, & t &\geq 0 \\
&= \ln |2z + 1| + \frac{2\sqrt{2}}{3\pi} |t|^{3/2}, & t &= 0 - .
\end{aligned} \tag{41}$$

This critical behavior is verified by numerical integrations whose results are shown in Fig. 6.

VII. SUMMARY

We have solved exactly a free-fermion vertex model in d dimensions. The vertex model is described by lines running in a preferred direction with the weights of vertices of intersecting lines prescribed by the free-fermion condition (2). The partition function (5) contains a fugacity -1 for each loop of lines and therefore consists of positive and negative weights. The per-site free energy is evaluated exactly in (10). The critical point is found to be given by (21) and the critical behavior given by $t^{(d+1)/2}$. In exceptional cases this critical behavior is modified with d replaced by an integer lower than the actual dimensionality.

This work has been supported in part by NSF Grants DMR-9313648 and INT-9207261.

REFERENCES

- [1] See, for example, R. J. Baxter, *Exactly solved Models in Statistical Mechanics* (Academic Press, London, 1982).
- [2] M. Suzuki, Phys. Rev. Lett. **28**, 507 (1972).
- [3] P. Orland, Int. J. Mod. Phys. B**5**, 2401 (1991).
- [4] H. W. J. Blöte and H. J. Hilhorst, J. Phys. A**15**, L631 (1982).
- [5] A. B. Zamolodchikov, JETP **52**, 325 (1980); Commun. Math. Phys. **79**, 489 (1981).
- [6] R. J. Baxter, Physica D**18**, 321 (1986).
- [7] V. V. Bazhanov and R. J. Baxter, J. Stat. Phys. **71**, 839 (1993).
- [8] F. Y. Wu and H. Y. Huang, Lett. Math. Phys. **29**, 205 (1993).
- [9] H. Y. Huang and F. Y. Wu, Physica A**205**, 31 (1994).
- [10] C. Fan and F. Y. Wu, Phys. Rev. **179**, 560 (1969).
- [11] C. Fan and F. Y. Wu, Phys. Rev. B**2**, 723 (1970).
- [12] J. E. Sacco and F. Y. Wu, J. Phys. A**8**, 1780 (1975).
- [13] P. W. Kasteleyn, Physica **27**, 1209 (1961).

FIGURES

FIG. 1. Decomposition of a vertex configuration of $2r$ incident bonds into $r!$ line configurations.

FIG. 2. A city of $2d$ points for $d = 3$.

FIG. 3. The correspondence between vertex configurations on \mathcal{L} and dimer coverings on \mathcal{L}' .

FIG. 4. Vertex configurations and weights for a 6-vertex model.

FIG. 5. Phase diagram of the three-dimensional model (30). Regimes I and II are in frozen states with $f_3 = 0$ and $f_3 = \ln |z_1|$, respectively.

FIG. 6. Results of numerical integrations of $df_3(z)/dz$ for the three-dimensional model (38).

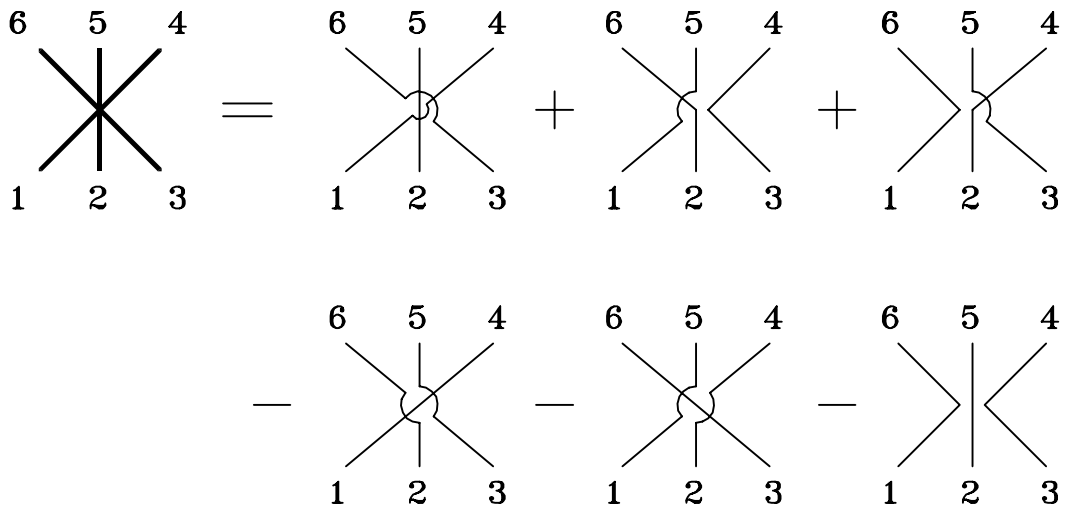


Fig. 1

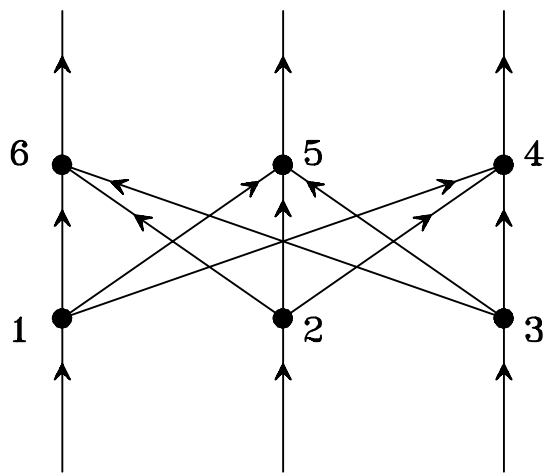


Fig. 2

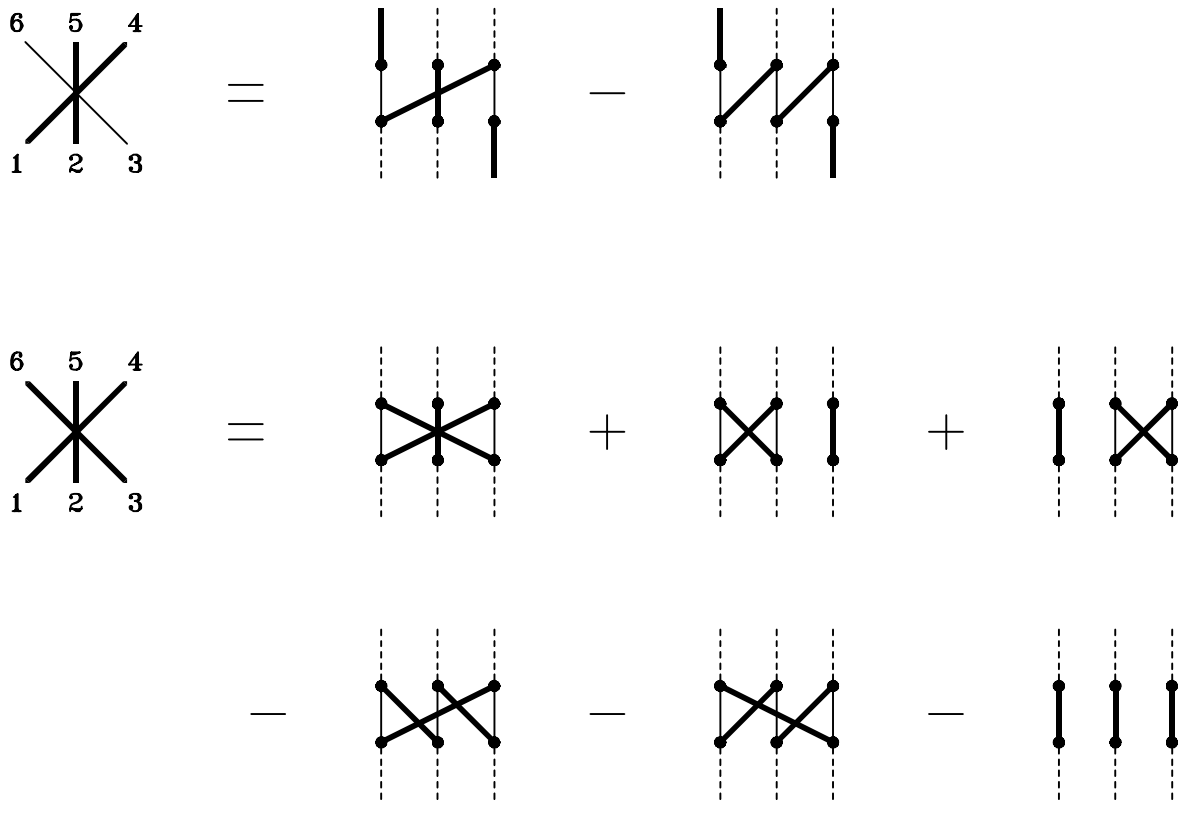


Fig. 3



Ω_1



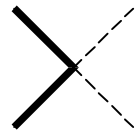
Ω_2



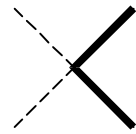
Ω_3



Ω_4



Ω_5



Ω_6

Fig. 4

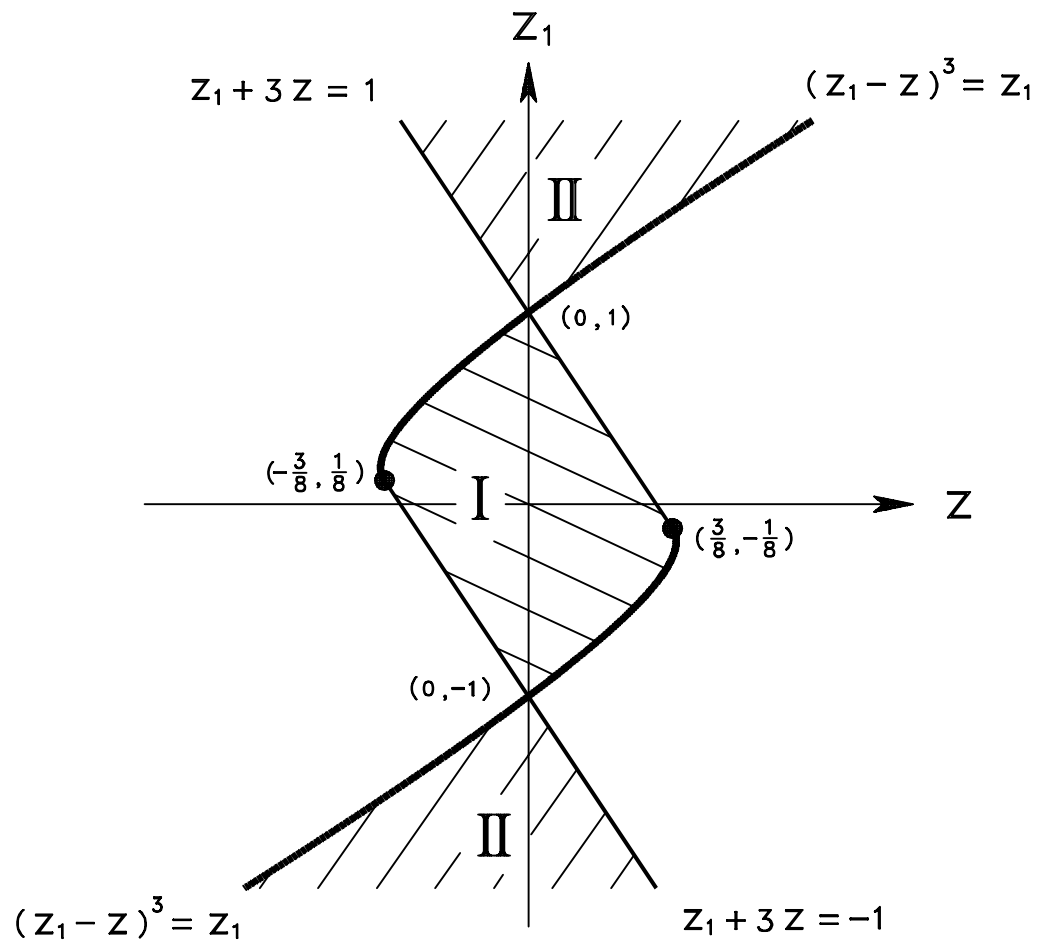


Fig. 5

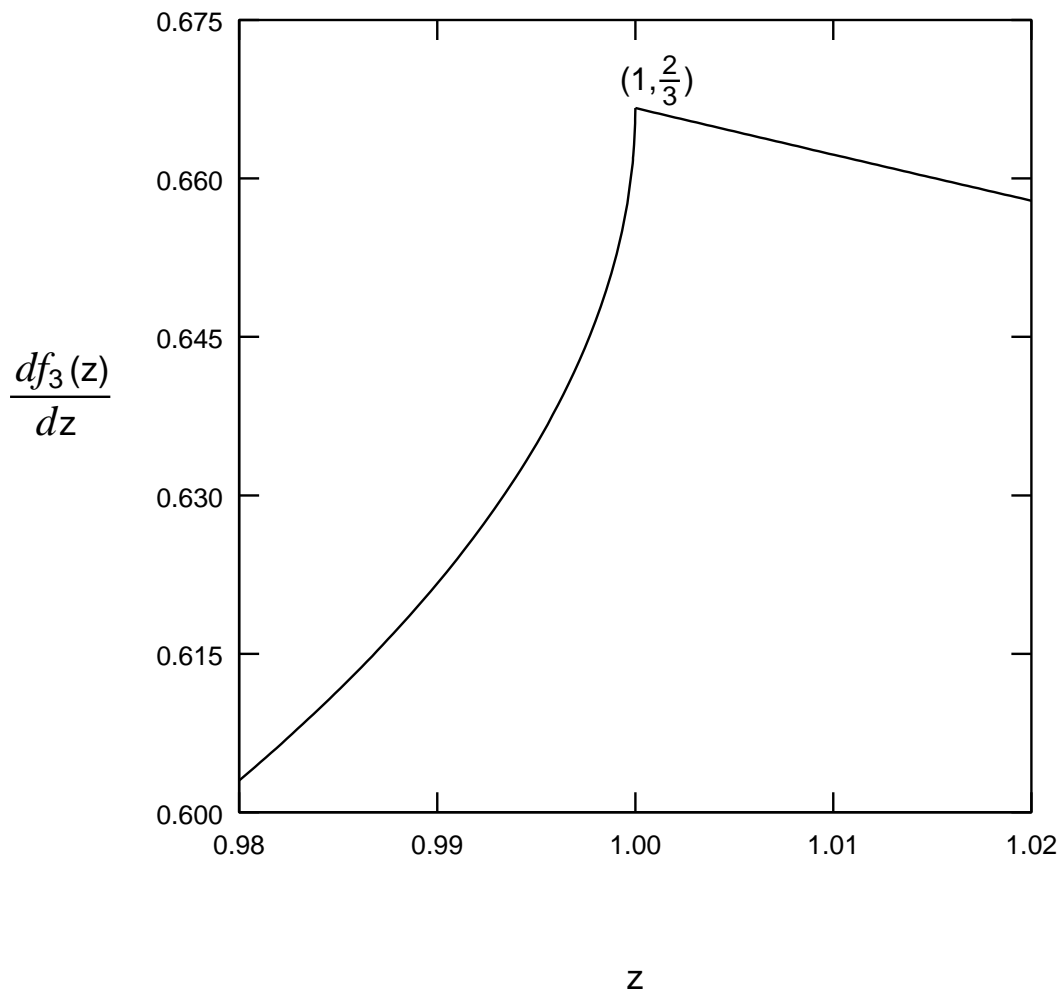


Fig. 6